BIOLOGY OF REPRODUCTION (2014) **90**(6):128, 1–14
Published online before print 16 April 2014.
DOI 10.1095/biolreprod.113.114447

Adenine Nucleotide Metabolism and a Role for AMP in Modulating Flagellar Waveforms in Mouse Sperm[1]

Melissa L. Vadnais,[5,6] Wenlei Cao,[3,5,6] Haig K. Aghajanian,[5,6] Lisa Haig-Ladewig,[6] Angel M. Lin,[6] Osama Al-Alao,[4,6] and George L. Gerton[2,6,7]

[6]*Center for Research on Reproduction and Women's Health, Perelman School of Medicine, University of Pennsylvania, Philadelphia, Pennsylvania*
[7]*Department of Obstetrics and Gynecology, Perelman School of Medicine, University of Pennsylvania, Philadelphia, Pennsylvania*

ABSTRACT

While most ATP, the main energy source driving sperm motility, is derived from glycolysis and oxidative phosphorylation, the metabolic demands of the cell require the efficient use of power stored in high-energy phosphate bonds. In times of high energy consumption, adenylate kinase (AK) scavenges one ATP molecule by transphosphorylation of two molecules of ADP, simultaneously yielding one molecule of AMP as a by-product. Either ATP or ADP supported motility of detergent-modeled cauda epididymal mouse sperm, indicating that flagellar AKs are functional. However, the ensuing flagellar waveforms fueled by ATP or ADP were qualitatively different. Motility driven by ATP was rapid but restricted to the distal region of the sperm tail, whereas ADP produced slower and more fluid waves that propagated down the full flagellum. Characterization of wave patterns by tracing and superimposing the images of the flagella, quantifying the differences using digital image analysis, and computer-assisted sperm analysis revealed differences in the amplitude, periodicity, and propagation of the waves between detergent-modeled sperm treated with either ATP or ADP. Surprisingly, addition of AMP to the incubation medium containing ATP recapitulated the pattern of sperm motility seen with ADP alone. In addition to AK1 and AK2, which we previously demonstrated are present in outer dense fibers and mitochondrial sheath of the mouse sperm tail, we show that another AK, AK8, is present in a third flagellar compartment, the axoneme. These results extend the known regulators of sperm motility to include AMP, which may be operating through an AMP-activated protein kinase.

ADP, AK8, AMP, ATP, adenine nucleotides, adenylate kinase, motility, sperm

INTRODUCTION

The mature spermatozoon is a highly defined and compartmentalized cell. The sperm consists of the head (containing the nucleus and acrosomal vesicle) and the flagellum, the specialized motile powerhouse of the cell. The canonical ''9 + 2'' microtubular axoneme runs down the center of the full length of the flagellum, which is delineated into three specialized structural compartments: the midpiece, the principal piece, and the end piece. The outer dense fibers (ODFs) are present throughout the midpiece and the principal piece. The midpiece is delineated by the presence of mitochondria wrapped in a spiral pattern around the nine ODFs that emanate from the outer doublets of the axoneme (9 + 9 + 2). At the distal end of the midpiece is the annulus, the demarcation point for the principal piece, characterized by the fibrous sheath. In this compartment, two longitudinal columns replace ODFs 3 and 8 and substitute for the mitochondria in encapsulating the seven remaining ODFs. The fibrous sheath functions as a scaffold for glycolytic enzymes and proteins in signaling pathways that regulate sperm maturation, motility, capacitation, hyperactivation, and/or acrosomal exocytosis [1]. The end piece is found at the tip of the flagellum and contains no structural elements other than the axoneme.

These structural considerations and the small amount of cytoplasm place a limit on the ability of sperm to carry much in the way of energy reserves. Furthermore, the length of the cells and compartmentalization of glycolysis and oxidative phosphorylation in the principal piece and the mitochondrial midpiece of the flagellum, respectively, pose daunting challenges for distributing ATP, the product of these processes, throughout the cell. The predicament of buffering adenine nucleotides (ATP and its congeners ADP, AMP, and cAMP) throughout the sperm cell is evident from the many roles these molecules play and the challenges posed by the strict compartmentalization of the sperm cell [1–3]. Adenine nucleotides are required from one end of the sperm to the other, providing energy and signaling molecules for motility and acrosomal exocytosis. ATP is the key phosphate donor for phosphorylation reactions carried out by protein kinase A (PKA) and tyrosine kinases during sperm capacitation [4]. ATP and cAMP are known to serve as ligands in important signaling steps or regulatory processes [5–7].

Adenine nucleotide buffering is accomplished throughout cells, in general, through the activity of adenylate kinases (AK) [8]. Adenylate kinases (AKs) catalyze the transphosphorylation reaction that reversibly rearranges two molecules of ADP to one molecule each of ATP and AMP ($2ADP \rightleftharpoons ATP + AMP$) [8]. Thus, when a cell is incapable of synthesizing adequate ATP under periods of extreme energy utilization, AK activity

[1]Supported by NIH grants R01HD051999, R01HD057144, T32HD007305, and P30ES013508.
[2]Correspondence: George L. Gerton, Center for Research on Reproduction and Women's Health, Department of Obstetrics and Gynecology, Perelman School of Medicine, University of Pennsylvania, 421 Curie Blvd., 1309 BRB II/III, Philadelphia, PA 19104-6160.
E-mail: gerton@mail.med.upenn.edu
[3]Current address: Department of Cell Biology, University of Massachusetts Medical School, Worcester, MA 01655-0002.
[4]Current address: Urology Department, Hamad General Hospital P.O. Box 3050, Doha, Qatar.
[5]These authors contributed equally to this work.

Received: 27 September 2013.
First decision: 5 November 2013.
Accepted: 19 March 2014.

eISSN: 1529-7268 http://www.biolreprod.org
ISSN: 0006-3363

can salvage energy from ADP. Years ago, this observation led Atkinson [8] to propose the concept of the ''adenylate energy charge'' theory, whereby most healthy and energy-stable cells maintained an energy charge (EC), defined by the equation EC = [(ATP) + 0.5(ADP)]/[(ATP) + (ADP) + (AMP)] in the range of 0.8–0.9. This concept was further supported by discoveries that when ATP is in high demand, the level of AMP, a by-product of the AK transphosphorylation reaction to produce ATP from ADP, rises. Furthermore, AMP itself can directly regulate enzymes in the glycolytic pathway, such as phosphofructokinase; indirectly affect energy-producing pathways by acting as a transcriptional regulator; and/or function as a second messenger activator of kinases [9–11]. It is also important to note that AMP can also be produced from the metabolic conversion of cAMP by cyclic nucleotide phosphodiesterase hydrolysis [12].

There are at least eight AK genes in the mouse. We previously demonstrated that multiple AK isoforms are compartmentalized within accessory structures of sperm flagella [3]. AK1, which is cytoplasmic in somatic cells, is found in association with the outer microtubular doublets and ODFs of the midpiece and principal piece of the sperm flagellum. AK2, a mitochondrial protein in somatic cells, is predictably restricted to the mitochondrial sheath of the sperm midpiece. AK1 and AK2 in the flagellar accessory structures provide a mechanism to buffer the adenylate energy charge for sperm motility. We also found that mRNAs encoding several other AKs are expressed in male mouse germ cells. Each of these enzymes may exist in specific compartments of the sperm to control precise cellular functions. In other laboratories, mutation of the evolutionarily conserved murine adenylate kinase 7 (*Ak7*) gene was found to produce pathological signs characteristic of primary ciliary dyskinesia, including ultrastructural ciliary defects, decreased ciliary beat frequency in respiratory epithelium, and defects in sperm flagella [13]. Furthermore, some proteins with other functions, such as the cystic fibrosis transmembrane regulator, a component of sperm, also have intrinsic AK activity [14].

With this background, our broad, long-term goal is to integrate adenine nucleotide metabolism into pathways of synthesis, degradation, and signaling in sperm. To assess AK function in sperm, we examined whether both ATP and ADP could support flagellar motion of detergent-modeled mouse sperm. We also probed the motility patterns fueled by these energy sources to see if they were different and, if so, why. In addition, we expanded our studies of members of the AK family in male germ cells and in cauda epididymal sperm. Protein studies of male mouse germ cells and Triton X-100-resistant and SDS-soluble structures of cauda epididymal sperm were carried out to determine if one of these members, AK8, associated with a particular compartment within mouse sperm.

MATERIALS AND METHODS

Isolation of Germ Cells

All animal procedures were approved by the University of Pennsylvania Institutional Animal Care and Use Committee. Mixed germ cells were prepared from decapsulated testes of adult male mice (Crl:CD1 [ICR] retired breeders; Charles River Laboratories) by sequential dissociation with collagenase and trypsin-DNase I [15]. To purify populations of pachytene spermatocytes, round spermatids, and condensing spermatids, the mixed germ cells were separated at unit gravity in a 2%–4% bovine serum albumin (BSA) gradient in Eagle essential medium with Earle salts [16, 17]. Both the pachytene spermatocyte and the round spermatid populations were at least 85% pure as determined by microscopic examination and differential counting with a hemocytometer; whereas the condensing spermatid population was approximately 40%–50% pure, with the balance being primarily anucleate residual bodies and round spermatids.

Sperm Extraction and Reactivation

Caudae epididymides of CD-1 retired breeders (Charles River Laboratories) were nicked with scissors, and the sperm were extruded into TYH medium incubated at 37°C in 5% CO_2 and air in a humidified incubator. As previously described, the sperm were allowed to swim out for 5 min in the incubator before a 50-μl aliquot was transferred to 450 μl of 37°C extraction medium (200 mM sucrose, 25 mM glutamic acid, 25 mM KOH, 0.10% Triton X-100, 20 mM HEPES, 1 mM DTT, pH 7.9) for 30 sec [5]. A 50-μl aliquot of this extracted sperm suspension was then transferred to 450 μl of reactivation medium (200 mM sucrose, 25 mM glutamic acid, 25 mM KOH, 1 mM EGTA, 4 mM $MgSO_4$, 20 mM HEPES, 0.01% PVA, 1 mM DTT, pH 7.9) containing ATP, ADP, and/or AMP 37°C (catalog numbers A9187, A2754, A1752; Sigma Chemical Co.). Samples of the reactivated sperm were transferred to prewarmed slides with 100-μm-depth chambers (Leja Products), observed with a Nikon inverted microscope, and recorded using a DAGE MTI 3CCD video camera at 30 fps.

Analysis of Sperm Motility

Tracing. For visual display of the wave patterns of motility fueled by ATP or ADP, individual frames from QuickTime movies were outlined on tracing paper placed over a computer monitor and superimposed at 0.06-sec intervals for a total of one cycle.

Angularity. Videos of the sperm were analyzed using the Macintosh computer graphic digitizer program GraphClick from Arizona Software (http://www.arizona-software.ch), which allows the automatic generation of the X-Y coordinates of positions on a line identified on a single image or successive, individual frames from a QuickTime movie. For sperm, equidistant positions, starting at the neck and progressing along the length of the flagellum, were marked, and their corresponding X and Y coordinates in a Cartesian plane were collected for each frame of a video at 0.03-sec intervals for a total of 5 sec (167 frames). To describe the wave characteristics in different regions of the sperm tail, angularity was measured at two regions of a flagellum in a series of images: [1] in the midpiece region near the head and [2] in the principal piece proximal to the annulus. Angularity was calculated by analyzing the triangle formed by connecting three successive points along the flagellum in each of these two regions as identified by GraphClick (illustrated in Fig. 3). The coordinates of the three vertices of each triangle—(X_1, Y_1), (X_2, Y_2), and (X_3, Y_3)—were used to calculate the distances (d_1, d_2, and d_3) between the three loci:

$$d_1 = \sqrt{(X_2 - X_1)^2 + (Y_2 - Y_1)^2} \quad (1)$$

$$d_2 = \sqrt{(X_3 - X_2)^2 + (Y_3 - Y_2)^2} \quad (2)$$

$$d_3 = \sqrt{(X_1 - X_3)^2 + (Y_1 - Y_3)^2} \quad (3)$$

Using these distances, the angles Θ_1, Θ_2, and Θ_3 were calculated by the use of the Law of Cosines:

$$\Theta_1 = \arccos({d_2}^2 + {d_3}^2 - {d_1}^2)/2d_2d_3 \quad (4)$$

$$\Theta_2 = \arccos({d_1}^2 + {d_3}^2 - {d_2}^2)/2d_1d_3 \quad (5)$$

$$\Theta_3 = \arccos({d_1}^2 + {d_2}^2 - {d_3}^2)/2d_1d_2 \quad (6)$$

Angularity (A) was then calculated with the equation

$$A = \sqrt{(\Theta_1)^2 + (\Theta_2)^2 + (\Theta_3)^2} \quad (7)$$

where the angles Θ_1, Θ_2, and Θ_3 are expressed in radians. For the purpose of spotting trends in the data over time, moving averages of the angularity values over three consecutive time points for each region (1–3 and 4–6) were plotted and overlaid on a graph.

CASA Statistics. Mouse sperm from caudae epididymides were isolated and detergent treated as described above. They were then reactivated in solutions containing 3 mM ATP, 3 mM ADP, or 3 mM ATP plus 1 mM AMP. CASA analysis was performed following the manufacturer's instructions and using the parameters detailed in Table 1. Detergent-permeabilized sperm did not

TABLE 1. The parameter settings used for CASA analysis (Hamilton Thorne IVOS software, version 12.2L).

Parameter	Measurement	Setting
Image capture	Frames per second	60 Hz
	Number of frames	60
Cell detection	Minimum contrast	80
	Minimum size	3 pixels
Progressive cells	Average path velocity (VAP)	25.0 μm/sec
	Straightness (SIR)	80.0%
Static cells	VAP cutoff	5.0 μm/sec
	VSL cutoff	11.0 μm/sec
Defaults	Cell size	6 pixels
	Cell intensity	160

uniformly become motile following addition of ATP or ADP, indicating that individual cells did not exhibit the same activation response. Since we were focused on the movement characteristics of single cell flagella, approximately 25 individual motile sperm tracks were selected from each CASA run to form the set of data for analysis. These experiments were performed on three separate dates and at three separate times on each date. The sperm motility parameters from each track were entered into the GraphPad Prism 4 statistics program to calculate and to graph the means and standard errors for each set of data. Statistical difference was determined with the Student *t*-test.

Intact cauda epididymal sperm were treated with agents that modify AMPK activity using either noncapacitating (modified Whitten medium: 109.5 mM NaCl, 4.7 mM KCl, 1.2 mM $MgSO_4{\cdot}7H_20$, 5.5 mM glucose, 1.2 mM KH_2PO_4, 0.23 mM sodium pyruvate, 4.8 mM L-[+]-lactic acid, hemicalcium salt, 0.01% polyvinylalcohol, 22 mM HEPES, 10 μg/ml Gentamicin, 0.001% phenol red) or capacitating (modified Whitten medium containing 10 mM $NaHCO_3^-$, 3 mM cyclodextrin) media [18]. The agents used were 5-aminoimidazole-4-carboxamide 1-β-D-ribofuranoside (AICAR; repeated five times at concentrations of 0 μM, 100 μM, 500 μM, and 2.5 mM); 9-β-D-arabinofuranosyladenine (Ara-A; repeated three times at concentrations of 0 μM, 100 μM, 300 μM, and 1.0 mM); Compound C (repeated twice at concentrations of 0, 0.1, 1, 10, and 100 μM); and metformin (repeated two times at concentrations of 0 μM, 400 μM, 2 mM, and 10 mM). At 0, 1, and 2 h of incubation, samples were collected for CASA (all agents) and tyrosine phosphorylation analyses (AICAR and Ara-A).

Preparation of RNA and PCR

Total RNA was prepared from spermatogenic cells, testis, ovary, oviduct, uterus, and various somatic tissues using Tri Reagent (Sigma). Messenger RNAs were then purified using the Dynabeads mRNA Direct Kit (Invitrogen) according to manufacturer's instructions. For RT-PCR, reverse transcription using 1 μg mRNA was performed using SuperScript II Reverse Transcriptase according to the manufacturer's instructions (Invitrogen). Products were amplified using Extaq DNA Polymerase (Takara Co.) and the appropriate primers (Table 2). Amplicons were sequenced at the University of Pennsylvania DNA Sequencing Facility. For quantitative RT-PCR assays, primers were designed using Primer Express 1.5 Taqman Primer Design software (Applied Biosystems) (Table 2). Products were amplified with the SYBR Green PCR Master Mix and analyzed with the ABI 7900 HT Sequence Detection system. The following PCR protocol was used: 1) denaturation (50°C for 2 min, 95°C for 10 min), 2) amplification and quantification (95°C for 15 sec, 60°C for 1 min) repeated for 40 cycles, 3) a dissociation curve program (95°C for 15 sec, 60°C for 15 sec, 95°C for 15 sec), and 4) cooling to 4°C. Amplicons were analyzed by generating a dissociation curve and determining the threshold cycle (Ct) value for each transcript. The relative quantification of gene expression was analyzed by the 2-DDCT method [19]. The mRNA corresponding to ribosomal protein S16 (accession no. BC082286) was used as a control [20].

Northern Blot Hybridization

Messenger RNA (0.5 μg each) from the mixed germ cells was separated by electrophoresis in a 1% agarose gel, containing formaldehyde, and transferred to Hybond N+ membranes (GE Healthcare). The probes were derived from the initial *Ak8* (accession no. NM_001033874) 318-bp PCR product and a 540-bp amplicon derived from *Rps16* (accession no. NM_013647; Table 2). Probes were ligated into a pCRII-TOPO vector (Invitrogen), sequenced, quantified by comparison to a *Hin*dIII ladder (New England Biolabs), and labeled with digoxigenin (DIG)-dUTP using in vitro transcription (DIG Northern Starter Kit; Roche). The probe was used for hybridization at 68°C for 2 h to Hybond N+ membranes. Membranes were washed to a stringency of 1× SSC (diluted from 20× SSC: 3 M sodium chloride, 0.3 M sodium citrate, pH 7.0) and then 0.05xSSC and 0.1% SDS up to 68°C. Immunological detection with anti-DIG antibody and chemiluminescence reaction with CDP-Star was used to assess the presence of *Ak8* and *Rps16* RNAs following manufacturer's instructions.

5′ and 3′ Rapid Amplification of cDNA Ends, Cloning of Ak8, and cDNA Sequence Analyses

Mixed germ cell amplicons, produced as described above, were cloned into a pCR2.1-TOPO vector (Invitrogen). Plasmid DNA was prepared and sequenced as directed by the manufacturer's instructions. The RLM-RACE kit (Ambion) was used for 5′ and 3′ rapid amplification of cDNA ends (RACE), and 1 μg of total RNA aliquots was used as a template for reverse transcription with the supplied 5′ (5′-GCU GAU GGC GAU GAA UGA ACA CUG CGU UUG CUG GCU UUG AUG AAA-3′) and 3′ (5′-GCG AGC ACA GAA TTA ATA CGA CTC ACT ATA GGT 12VN-3′) RACE adapters. The cDNA was then subjected to PCR using the 5′ (5′-GCT GAT GGC GAT GAA TGA ACA CTG-3′) and 3′ (5′-GCG AGC ACA GAA TTA ATA CGA CT-3′) RACE primers, which were complementary to the anchored adapter, and a primer specific for *Ak8* (Table 2). Gradient PCR was used to optimize annealing temperatures. All PCR products were sequenced in both directions. The cloned sequences were analyzed using MacVector Software v12.0.3 (MacVector Inc.).

Generation of AK8 Antibody

Antiserum was generated by immunizing rabbits against AK8 using two peptides (Peptide 1: MDATTAPHRIPPEM–C [1–14]; Peptide 2: C-VQVRLLQNPKDSEEYIK [414–430]; Quality Controlled Biochemicals). Preimmune serum was tested using SDS-PAGE and immunoblotting techniques to ensure antibody specificity. To confirm AK8 antiserum specificity, anti-AK8 serum was preabsorbed with 10:1 molar ratios of Peptide 1, Peptide 2, or both Peptide 1 and Peptide 2 and then evaluated using SDS-PAGE and immunoblotting.

TABLE 2. Primer sequences used to analyze the expression of *Ak8*.

Name of primer	Application	Sequence (5′-3′)
Ak8 primer set 1: forward	RT-PCR	CAG AAC CCC AAG GAT TCA GA
Ak8 primer set 1: reverse	RT-PCR	CCT GGG CAG AGG ATT AAT GA
Ak8 primer set 2: forward	RT-PCR	GCG TCT GAA TGA AGA TGA CTG CC
Ak8 primer set 2: reverse	RT-PCR	AGA ATC CTG ATG ATG TGC CTG TG
Ak8 full-length sequence: forward	RT-PCR, RACE Northern probe	ACT AAG GAG CGG AGC GCT GTC G
Ak8 full-length sequence: reverse	RT-PCR, Northern probe	TTG AGG GCA GGG GCT TTG AAT G
Ak8: forward	qRT-PCR	TGT CAC CGG AGA GAT CTA TCA CA
Ak8: reverse	qRT-PCR	CCG TTT CGA TCT CCG AGA TG
Rps16: forward	Northern probe	CCT GAA AAA TCG GCT GGG TTG
Rps16: reverse	Northern probe	CTT GAG ATG GGC TTA TCG GTA GG
Gapdh: forward	RT-PCR	AAC TTT GGC ATT GTG
Gapdh: reverse	RT-PCR	GGA TGC AGG GAT GAT

Purification and Detergent Fractionation of Cauda Epididymal Sperm

Sperm were collected by cutting the caudae epididymides of male mice and extruding the sperm at 37°C into phosphate-buffered saline (PBS: 2.68 mM KCl, 136.09 mM NaCl, 1.47 mM KH_2PO_4, 8.07 mM Na_2HPO_4, pH 7.4 containing protease inhibitors [catalog no. 1 1697498001, Roche Applied Science]). The sperm were collected by centrifugation at 800 × *g* for 5 min at room temperature, resuspended in PBS at 4°C, and counted.

For detergent fractionation, 1×10^5 cauda epididymal sperm in 100 µl of PBS at 4°C were incubated on ice for 10 min and then centrifuged at 10 000 × *g* at 4°C for 1 min. Ice-cold PBS extractable and nonextractable proteins were collected from the supernatant and pellet, respectively. Cells (10^5) in 100 µl of PBS containing 0.1% Triton X-100 were incubated at room temperature for 10 min and then centrifuged at 10 000 × *g* for 1 min. Triton X-100-soluble and -insoluble proteins were collected from the supernatant and pellet, respectively. Further detergent extraction was performed on the Triton X-100-insoluble proteins (pellets). One hundred microliters of S-EDTA (1% SDS, 75 mM NaCl, 24 mM EDTA, protease inhibitors [Roche], pH 6.0) were added to the Triton X-100-insoluble protein pellet, incubated at room temperature for 10 min, homogenized, and centrifuged at 10 000 × *g* for 1 min. The Triton X-100/S-EDTA-soluble and -insoluble proteins were collected from the supernatant and the pellet, respectively.

Protein Extraction and Immunoblot Analysis

Spermatogenic cells and sperm cells were concentrated by centrifugation, washed in 1 ml of PBS, resuspended in sample buffer (58 mM Tris-HCl, pH 6.8, 1.7% SDS, 6% glycerol), and boiled for 5 min. Detergent extracted proteins were mixed with sample buffer and boiled for 5 min. Other tissues were homogenized, sonicated, and boiled in the sample buffer. After centrifugation, the supernatants were recovered and saved. Protein concentrations were determined by the Micro-BCA Protein Assay Kit (Pierce Chemical Co.), and then dithiothreitol (DTT) and bromophenol blue were added to final concentrations of 100 mM and 0.002%, respectively. The samples were boiled for 5 min, and protein samples (15 µg per lane) were separated by SDS-PAGE in 10% polyacrylamide gels [21]. The gels were then transferred to polyvinylidene difluoride membranes [22]. After the membranes were blocked with TBST (125 mM NaCl, 25 mM Tris-HCl, pH 8.0, 0.1% Tween 20) containing 5% nonfat dry milk, they were incubated with primary antibody for 1 h (1:1000 AK8 antiserum). After washing with TBST, the blots were incubated for 1 h with secondary antibody (1:5000 alkaline phosphate-conjugated goat anti-rabbit IgG whole antibody [GE Healthcare] in 5% nonfat dry milk in TBST), and, after washing with TBST, the bound enzyme was developed with ECL Western Blotting Reagent Pack (GE Healthcare) according to the manufacturer's directions. A negative control using preimmune serum alone was used to check for specificity.

AMPK was examined in whole and detergent-modeled sperm. For the former, SDS-PAGE gels of whole cell protein were transferred to nitrocellulose membranes (Hybond-ECL; Amersham Biosciences) [22], blocked in Tris-buffered saline-Tween (TBST; 25mM Tris-HCl, pH 8.0; 125 mM NaCl; 0.1% Tween 20) containing 5% BSA and incubated with 45 ng/ml polyclonal rabbit anti-AMPKα affinity-purified antibody (catalog no. 2532; Cell Signaling) in 5% BSA in TBST overnight at 4°C. After a TBST wash, the blots were incubated with a secondary antibody (donkey anti-rabbit horseradish peroxidase-linked whole antibody; GE Healthcare) 1:5000 in 5% BSA in TBST, developed with an advanced enhanced chemiluminescence (A-ECL) kit (GE Healthcare), and exposed to film. To test whether AMPKα was present in the detergent-modeled sperm, 1×10^6 sperm were incubated in 50 µl of extraction medium for 30 sec and centrifuged, and the pellet and supernatant were separated. Fifty microliters of 1× sample buffer (62.5 mM Tris-HCl, pH 6.8, 1.67% SDS, 5% glycerol, 100 mM DTT, and 0.002% bromophenol blue) were added to the pellet, and 10 µl of 6× sample buffer were added to the supernatant. The samples were then sonicated on ice, boiled for 5 min, sonicated again, and centrifuged. The samples were then separated by SDS-PAGE in 10% Tris-HCl polyacrylamide gels and analyzed by immunoblotting as described above.

Indirect Immunofluorescence Analysis

Cauda epididymal sperm (10^6) were collected as described above, attached to polylysine-coated coverslips for 15 min, fixed with 4% paraformaldehyde in PBS for 15 min, and then permeablized with methanol for 2 min at −20°C. After extensive washing with PBS, the coverslips were incubated at room temperature for 30 min with 10% normal goat serum in PBS (blocking solution). Coverslips were incubated at 37°C for 1 h with primary antibody (1:25 AK8 antiserum) diluted in blocking solution. After washing with PBS, the coverslips were incubated for 1 h at 37°C with Alexa Fluor 488-conjugated goat anti-rabbit IgG (H+L) secondary antibody (1:100; Life Technologies) diluted in blocking solution. Finally, the coverslips were mounted on slides using 15 µl of Fluoromount-G (Southern Biotechnology Associates), observed with a Nikon Eclipse TE 2000-U inverted microscope (Nikon Instruments), and photographed with a CFW-1610C digital FireWire camera (Scion) using the NIH ImageJ imaging software available online (http://rsb.info.nih.gov/ij). Nomarski differential interference contrast micrographs were photographed in parallel with the fluorescence images. A negative control using preimmune serum alone was used to check for specificity.

RESULTS

ATP and ADP Can Support Sperm Motility

We previously demonstrated that AK isozymes are localized in detergent-resistant compartments of the sperm (e.g., mitochondria [AK2] and ODFs [AK1]) [3]. To test whether AK activity was capable of supporting sperm motility by conversion of ADP to ATP, we demembranated cauda epididymal mouse sperm with 0.1% Triton X-100 and incubated the sperm with individual adenine nucleotides or ADP with an AK inhibitor. Without an exogenous energy source, the resulting sperm cells became straight and immotile based on microscopic observation (not shown). When these sperm were placed in a reactivation solution containing 3 mM ATP, they regained motility (Fig. 1A; Supplemental Movie S1; Supplemental Data are available online at www.biolreprod.org). The addition of a reactivation solution containing 3 mM ADP was also able to rescue motility in these ''detergent-modeled'' sperm (Fig. 1B; Supplemental Movie S2). The inclusion of the specific inhibitor of AKs, Ap5A, in the ADP reactivation solution effectively blocked motility, demonstrating that ADP was fueling detergent-modeled sperm motility through its conversion to ATP by AK. AMP was not able to rescue motility (data not shown). Even though both ATP and ADP were able to rescue and support the motility of extracted sperm, the resulting wave patterns from the two conditions were notably different.

Reactivated Modeled Sperm Show Qualitatively Different Wave Patterns with ATP or ADP

On initial observation, sperm reactivated with ATP exhibited a motility pattern characterized by a ''whipping'' principal piece with a relatively rigid midpiece; as a consequence, the movement of the anterior part of the sperm was spasmodic. In contrast, sperm reactivated with ADP exhibited a more fluid, sinusoidal-like wave that propagated along the complete length of the tail. At 0.06-sec intervals, we traced outlines of sperm reactivated either with ATP or ADP through one cycle and superimposed the images (Fig. 2). The tracing of the sperm reactivated with ATP corroborated our initial observation of a stiff midpiece, with considerable more movement in the distal region of the flagellum. The waveform of this reactivation in the presence of ATP completed one cycle in approximately 0.23 sec (Fig. 2, left panel). Sperm reactivated with ADP exhibited a significantly longer cycle of 0.66 sec (Fig. 2, right panel). The sinusoidal nature of the ADP-reactivated tail motion waveform, illustrated in the right panel of Figure 2, had the property of a standing wave with discrete nodes and antinodes. The differences illustrated by comparing the tracings were compelling but nonetheless subjective and revealed the need for a method of objective analysis.

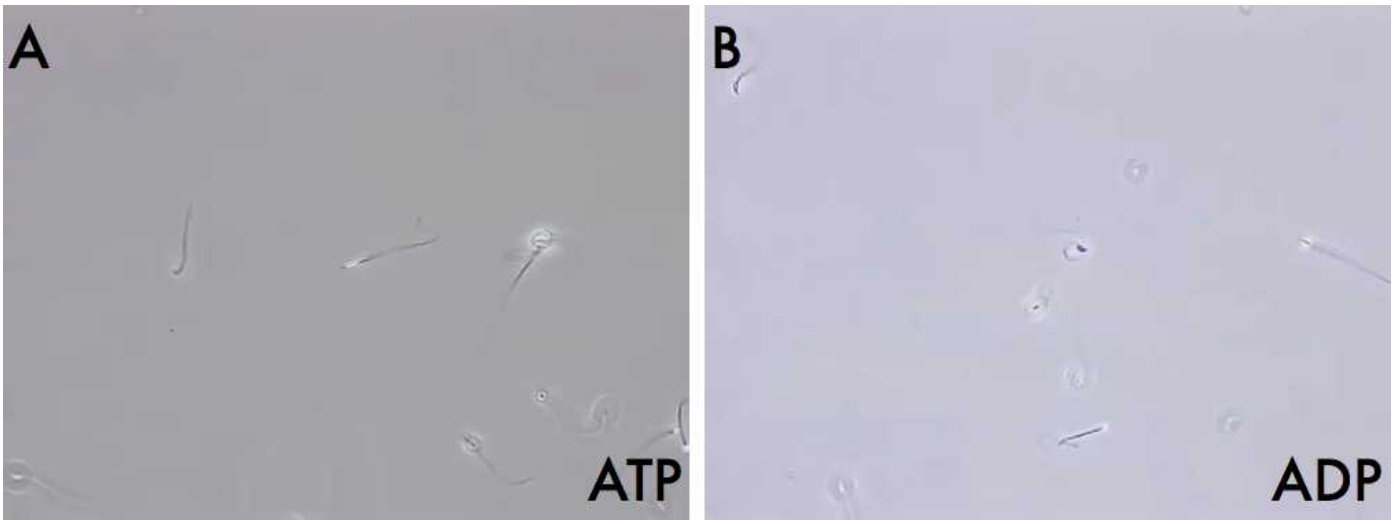

FIG. 1. Motility of detergent-modeled sperm reactivated by the addition of ATP or ADP. Shown are still images from video recordings at ×60 magnification (see Supplemental Movies S1 and S2) of detergent modeled sperm reactivated with solutions containing either ATP (**A**) or ADP (**B**).

Reactivated Modeled Sperm Exhibit Quantitatively Different Flagellar Movement (Angularity) with ATP or ADP

To quantify our observations, we developed a method to measure the differences between the patterns of motility seen in the ATP and ADP reactivation experiments. Using computer imaging software, the X and Y coordinates were recorded every 0.03 sec for 5 sec at discrete intervals along the flagellum of individual reactivated sperm. Using the coordinates of three positions approximating the midpiece (1, 2, 3) and three loci in the proximal end of the principal piece (4, 5, 6) we created two triangles and, using the equation described in the *Materials and Methods*, calculated the angularity (*A*) for each time point of the two regions (Fig. 3, A–C). For illustrative purposes, representative sperm reactivated with ATP or ADP were selected, and the moving averages of the angularity values over three consecutive time points for each region (1–3 and 4–6) were plotted and overlaid on a graph (Fig. 3, D and E).

Sperm reactivated with ATP showed less variation in angularity (and therefore movement) of the midpiece compared to the principal piece. In general, these sperm also had significantly less variation in angularity when compared to sperm reactivated with ADP. The sperm reactivated with ADP exhibited a constant variation of angularity between these two regions and a longer periodicity when compared with the ATP reactivated sperm. The forms of the waves from the proximal and distal regions of the ADP-reactivated sperm were very similar in amplitude and periodicity and showed a phase-shift consistent with a wave moving down the tail of the sperm.

AMP Modulates ATP-Reactivated Modeled Sperm Motility to Mimic That Seen with ADP

Although calculating angularity was effective in showing quantitative differences between the flagellar movements seen by reactivating sperm with either ATP or ADP, this method was very time consuming and able to analyze only one cell at a time. A method with a higher throughput, capable of simultaneously monitoring several motility parameters, was needed for a more accurate statistical analysis of the effects of

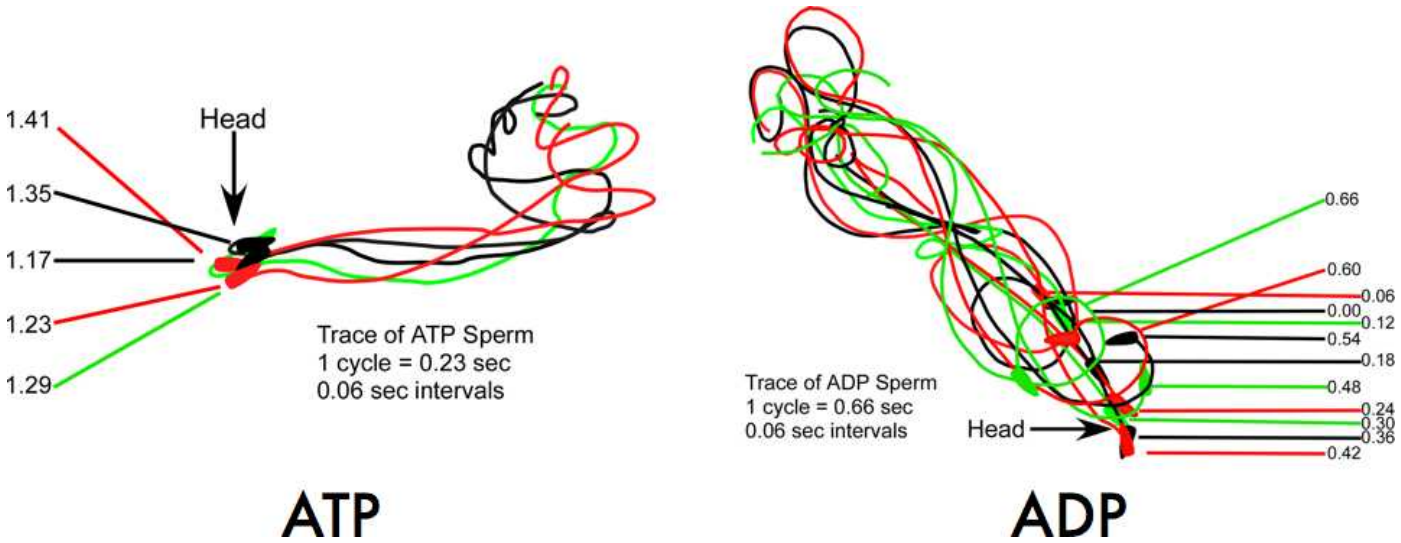

FIG. 2. Tracings of individual sperm reactivated by either ATP or ADP. Sperm were reactivated with ATP (left panel) or ADP (right panel) and captured on video. At 0.06-sec intervals, the flagella were traced from individual frames of the video.

ADP and ATP on the detergent-modeled sperm flagella. The use of the Hamilton-Thorne IVOS Computer Assisted Semen Analysis (CASA) system enabled us to analyze many sperm simultaneously, quickly, and efficiently. CASA also provided an objective description of the motility patterns observed with additional movement parameters (Fig. 4).

As shown in Figure 3, ADP activation created a wave that traveled down the complete length of the sperm but at a slower cycling rate compared to that obtained with ATP. When analyzed by CASA, ADP-reactivated sperm recorded significantly higher average values of amplitude of lateral head movement (ALH; Fig. 4) as well as lower beat cross frequency (BCF; Fig. 4) compared to ATP-reactivated sperm. The speed of the sperm as recorded by both curvilinear (VCL; Fig. 4) and straight-line velocities (VSL; Fig. 4) was faster in the sperm reactivated with ADP. The ratio of VSL to VCL, known as linearity (LIN; Fig. 4), was similar in the ATP- and ADP-reactivated sperm. These values are what one would predict from the visual inspection of the sperm performed for Figures 1 and 2.

In the reactivation experiments above, ATP was able to support sperm motility directly while ADP fueled sperm motility by its interconversion to ATP and AMP by AK (2 ADP $\rightleftharpoons$ ATP + AMP). Because both ATP and ADP reactivations used ATP as the final energy source for flagellar movement, the differences in visual observations, angularity, and CASA values between ADP- and ATP-reactivated sperm led us to hypothesize that AMP, the by-product of ADP conversion to ATP, regulated motility parameters. To test this hypothesis, detergent-modeled sperm were reactivated in the presence of ATP with or without added AMP, and motility patterns were analyzed by CASA (Fig. 4; ATP/AMP bar). These results demonstrated that the addition of AMP to the ATP reactivation medium recapitulated the detergent-modeled sperm motility pattern seen with ADP. Thus, AMP, in addition to being a by-product of the AK reaction, altered motility parameters in reactivated sperm through an unknown mechanism.

Mouse Sperm Contain a Target of AMP Action: AMP-Activated Kinase

We suspected that the difference in motility patterns between ATP- and ADP-fueled motility resulted from a regulatory property of AMP as opposed to a metabolic function. Although evidence was lacking for mouse sperm, AMP does act as a regulator of physiological functions in somatic cell systems through its role as a ligand for AMP-activated kinase (AMPK) [10]. We tested the possibility that AMPK is present in mouse cauda epididymal sperm by immunoblotting. A rabbit polyclonal antibody against the catalytic subunit of AMPK (AMPKα) detected a single, clear band at the appropriate molecular weight (62 000 M_r) in whole sperm protein extracts (Fig. 5). Furthermore, detergent-modeled sperm exhibited a similar band, confirming that AMPKα remained in the particulate compartment of sperm after Triton X-100 treatment. This procedure released only a negligible amount of AMPKα into the supernatant from the detergent-modeled sperm. Unfortunately, we were unable to use this antibody to localize the AMPKα protein in mouse sperm by indirect immunofluorescence.

We tested the involvement of AMPK in the AMP modification of the ATP-driven motility by looking to see if there were any differences between the phosphorylation state of AMPKα in detergent-modeled sperm and whether AICAR, Ara-A, Compound C, or metformin had any effect on the

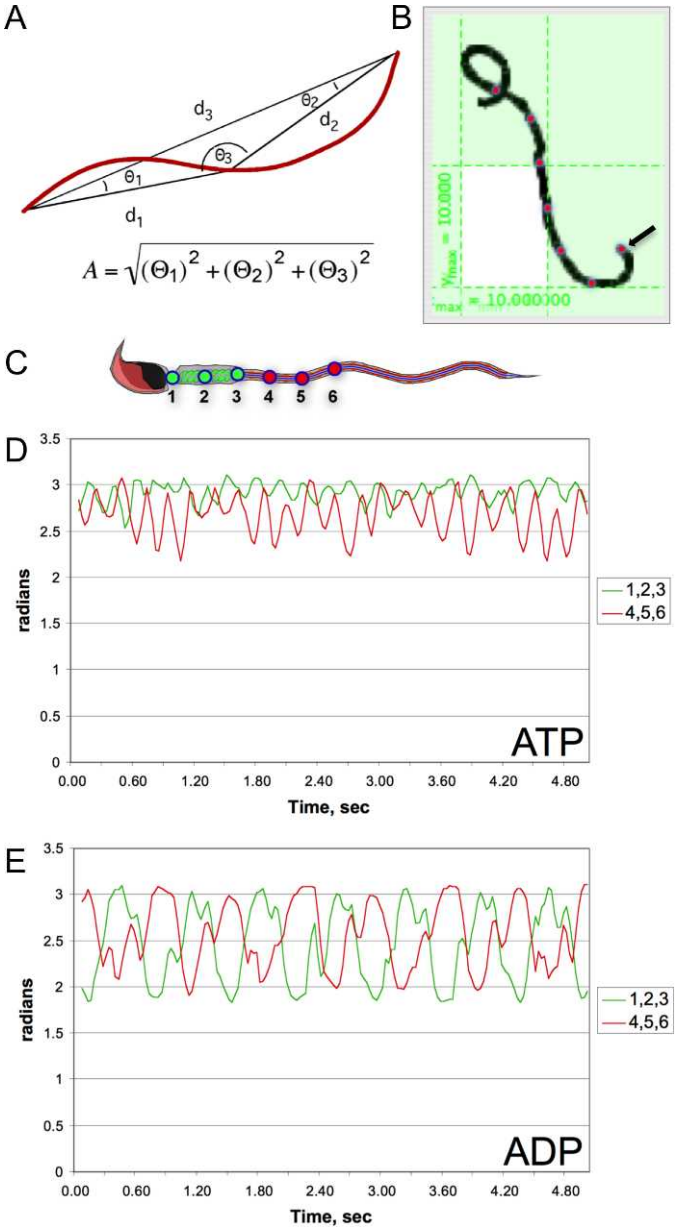

FIG. 3. Plots of angularity calculations at two different points in the flagella of detergent-modeled sperm reactivated with either ATP or ADP. Angularity was calculated by analyzing the triangle (**A**) formed by connecting three successive, equidistantly spaced points along the flagellum in two regions: 1) the midpiece and 2) the proximal principal piece. The points and their X and Y coordinates were identified with the program GraphClick (**B**). For a representative sperm reactivated with ATP or ADP, X and Y coordinates were recorded for points 1–3 (corresponding to the midpiece, as seen in green in **C**) and 4–6 (corresponding to the proximal region of the principal piece, depicted in red) every 0.03 sec for 5 sec. The angularities of these regions were calculated for each time point and plotted on graphs comparing the angularity of the midpiece to that of the principal piece of sperm reactivated with ATP (**D**) or ADP (**E**). Traces in green represent the midpiece region, and the traces in red correspond to the proximal region of the principal piece, plotted as a moving average over time (see *Materials and Methods* for detail).

motility patterns assessed by CASA or protein tyrosine phosphorylation of cauda epididymal sperm. We looked at the motility and tyrosine phosphorylation patterns of the sperm incubated under noncapacitating and capacitating conditions in the presence of AICAR, Ara-A, Compound C, and metformin and found no effect compared to controls (not shown). In

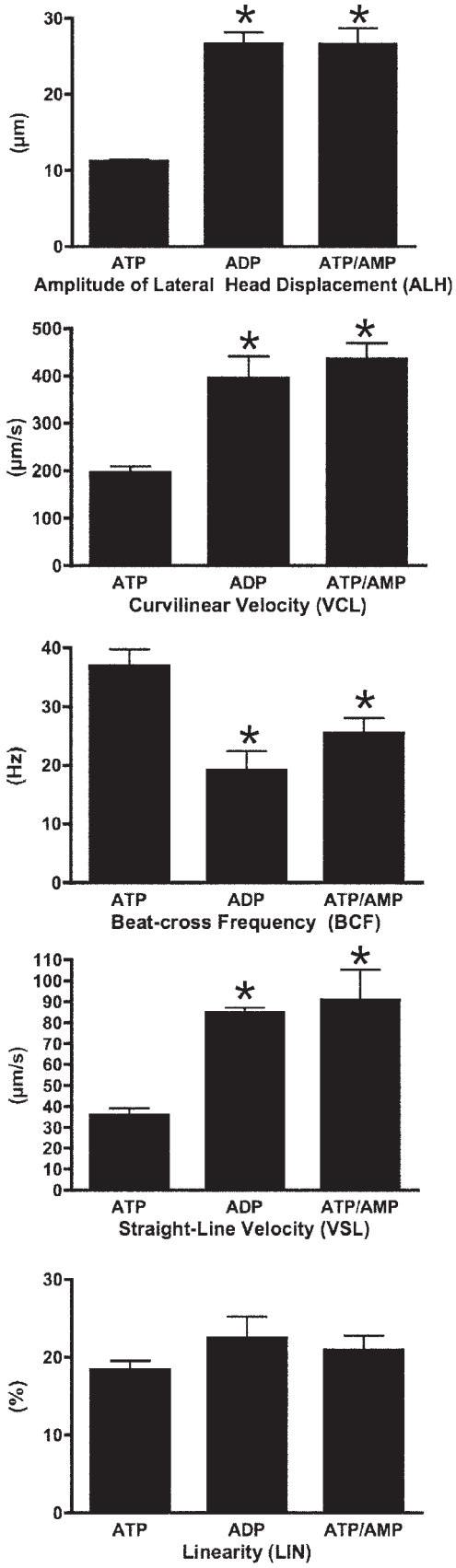

FIG. 4. CASA analysis of sperm motility parameters among sperm reactivated with ATP, ADP, or ATP plus AMP. Cauda epididymal sperm were collected, extracted with Triton X-100; reactivated in the presence of millimolar amounts of ATP, ADP, or ATP plus AMP; and analyzed by CASA. Values for amplitude of lateral head displacement (ALH), curvilinear velocity (VCL), beat cross frequency (BCF, representing the rate at which the sperm head crosses the average path of the moving sperm), straight-line velocity (VSL), and linearity (LIN, derived from the ratio VSL/VCL) were recorded, averaged, and graphed with the corresponding error bars. For ALH, VCL, BCF, and VSL, there is a significant difference between the values for ATP and ADP treatment as well as between the values for ATP and ATP/AMP treatments (asterisks, $P < 0.05$). There is no significant difference between the values for ADP and ATP/AMP treatments for ALH, VCL, BCF, and VSL. For LIN, there is no significant difference between the values for ATP and ADP as well as ATP and ATP/AMP.

addition, the inclusion of AMP in the reactivation medium did not alter the phospho-AMPKα immunoblot pattern of proteins from sperm treated with ADP or ATP.

The Ak8 *Expression Profile Is Consistent with Flagellar Expression*

In our earlier study, we found AK mRNA (called Ak_Riken; accession no. NM_001033874) in mixed germ cells from the mouse testis but not the brain [3]. After the publication of that paper, Ak_Riken was identified as Ak8. Homology searches suggested that AK8 is orthologous to AK58, an axonemal, dual AK domain protein found in Ciona sperm. RT-PCR, Northern hybridization, and RACE were utilized to determine the sequence and transcript length of Ak8 in mouse spermatogenic cells. A 318-bp PCR fragment in the coding region of Ak8 was amplified from mixed germ cell cDNA and confirmed by sequencing (not shown). Northern hybridization indicated that the Ak8 transcript size was 1.7–1.8 kb (not shown). Amplicons were produced by 5′ RACE and 3′ RACE, found to overlap, and verified by RT-PCR using primers designed from the full-length sequence (not shown). The sequence of the 1524-bp PCR amplicon matched the predicted RACE Ak8 sequence.

RT-PCR was used to determine which tissues expressed Ak8 and at what levels it was present in spermatogenic cells. Quantitative RT-PCR indicated that Ak8 mRNA expression gradually increased during spermatogenesis. The mRNA level in condensing spermatids, when the sperm flagellum is present, was 3.55-fold higher than that in pachytene spermatocytes, which lack a flagellum (Fig. 6A). RT-PCR produced a 170-bp Ak8 amplicon in all tissues examined when Ak8 primer set 1 was used, which is located in the 3′ UTR of the Ak8 sequence. However, when primer set 2 was used, which is located in the open reading frame, a 318-bp Ak8 amplicon was seen only in oviduct and testis (Fig. 6B). RT-PCR of Gapdh was used as a loading control (product size: 233 bp).

The AK8 Protein Contains Two AK Domains and Is Rich in Proline

AK8 has a theoretical size of 55 072, which approximates twice the values for AK1 and AK2. The doubling in size is due to the fact that AK8 contains two AK domains (Fig. 7). The protein also has a predicted alkaline isoelectric point of 8.34 (Table 3). Overall, the protein is rich in leucine (11.06%) and isoleucine (7.93%). In addition, proline is the third most abundant amino acid (7.72%). These residues are distributed throughout the sequence, and they are often conserved between the two AK domains. Figure 7 indicates the position of the AK consensus pattern of [LIVMFYWCA]-[LIVMFYW](2)-D-G-[FYI]-P-R-x(3)-[NQ] (http://prosite.expasy.org/PDOC00104) [23]. According to this website, the arginine (R) in this region is an active site residue; it is present in the both AK domains of

AK8. The website also indicates that the aspartate (D) in this consensus pattern is involved in a salt bridge; in the case of AK8, the D is present in the first AK domain of AK8, but it is substituted by a histidine (H) in the second AK domain. Besides the nucleotide binding pockets for AMP, ADP, and ATP, no other prominent domains were obvious when performing standard domain searches.

AK8 Is Present in Spermatogenic Cells with Flagella and Cauda Epididymal Sperm

An antiserum that recognizes the mouse AK8 protein was produced for use in immunoblotting and indirect immunofluorescence. The AK8 antiserum recognized a single protein band at the expected size of Mr 56 000, while preimmune serum did not detect any band (not shown). When the anti-AK8 serum was preabsorbed with the two peptide immunogens (Peptide 1, Peptide 2, or a mixture of Peptide 1 and Peptide 2) to confirm the specificity of the produced antiserum, the signal was significantly decreased compared to anti-AK8 serum alone (not shown).

SDS-PAGE and immunoblotting of spermatogenic cells and various tissues was performed to determine the AK8 protein expression profile. AK8 antiserum recognized proteins in mixed germ cells, round spermatids, and condensing spermatids (Fig. 8A). This is consistent with the results from quantitative RT-PCR. This antiserum also recognized protein in all tissues examined except liver (Fig. 8B). When the preimmune serum was used, no antigen was detected.

AK8 Localizes to the Flagellum of Cauda Epididymal Sperm

Indirect immunofluorescence was performed on cauda epididymal sperm to determine where AK8 was present. Probing with AK8 antiserum demonstrated that the protein was present along the full length of sperm tail and also in the acrosomal region of the sperm head (Fig. 9A). Sperm probed with preimmune serum did not display fluorescence (Fig. 9B). Attempts to use this antibody to localize the protein by immunoelectron microscopy were unsuccessful. The presence of the protein along the full length of the flagellum suggests that this protein is associated with the ODFs or axoneme. To resolve this issue, we resorted to differential detergent extraction of the sperm.

AK8 Is Associated with the Axonemes of Cauda Epididymal Sperm

Cauda epididymal sperm proteins were extracted with ice-cold PBS, Triton X-100, or Triton X-100 followed by S-EDTA. The resulting fractions were analyzed by SDS-PAGE and immunoblotting with AK8 antiserum to assess with which flagellar structures AK8 associated. Ice-cold PBS should only release loosely associated proteins, whereas Triton X-100 solubilizes sperm membranes and releases soluble cytoplasmic components but leaves the acrosomal matrix, nucleus, flagellar accessory structures, and axoneme intact. S-EDTA dissociates the sperm head from the flagellum. The axoneme is dissolved, leaving behind flagellar accessory structures such as the fibrous sheath, ODFs, and remnants of the mitochondrial sheath [24]. The AK8 antiserum recognized bands from the pellets remaining after ice-cold PBS or 1% Triton X-100 treatment (Fig. 10), and AK8 was not solubilized under these conditions. In contrast, AK8 was present in the supernatant of sperm extracted with 1% S-EDTA. Only a small amount remained in the pellet of this extraction (Fig. 10). This result is consistent with the association of AK8 with the axoneme since the ODFs are resistant to this extraction method, whereas the axoneme is solubilized [25].

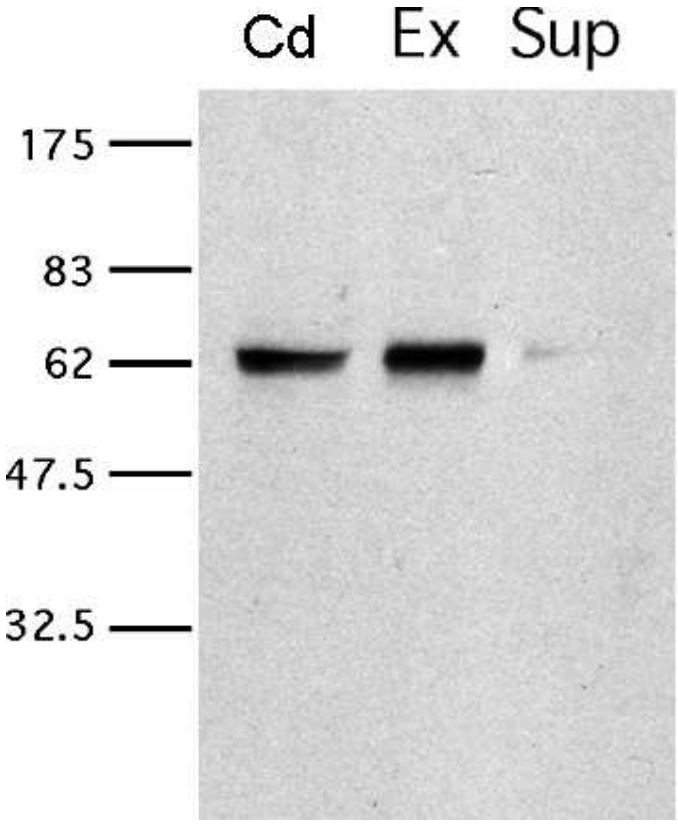

FIG. 5. Detection of AMPKα is present in both intact and detergent-modeled sperm. Protein extracts from intact mouse cauda epididymal sperm (Cd), detergent-extracted sperm (Ex), and the supernatant following detergent treatment (Sup) were analyzed by immunoblotting using a rabbit polyclonal anti-AMPKα antibody. Each band detected in Cd and Ex is the expected size for AMPKα. The numbers on the left represent molecular weights of standard proteins ($\times 10^{-3}$).

DISCUSSION

We have shown here for the first time that AMP produced by AK has profound effects on the motility patterns of detergent-modeled mouse sperm. Although it has been known for many years that ADP can be converted to ATP by AK-catalyzed transphosphorylation and subsequently used to fuel sperm motility [26–28], the results presented here are the first to demonstrate a direct effect of AMP on the wave frequency, amplitude, and motility pattern of the detergent-extracted sperm. As described below, these findings also explain previous observations that were attributed to ADP alone.

Almost four decades ago, ADP was shown to affect the motility pattern of detergent-treated bull sperm in a manner different from ATP [26]. In the presence of 1 mM ATP alone, the bovine sperm exhibited a jittering, uncoordinated movement, but the pattern of motion could be converted to a more rhythmic beating by the inclusion of ADP. In this previous article, ATP was reported to be capable of supporting motility in detergent-extracted bovine sperm, but under the conditions of the study, motion requires mechanical initiation, whereas ADP-induced motility requires no initiation, and the pattern observed appears similar to that of intact cells [26]. Recently, Lindeman et al. [26] revisited this phenomenon and found that

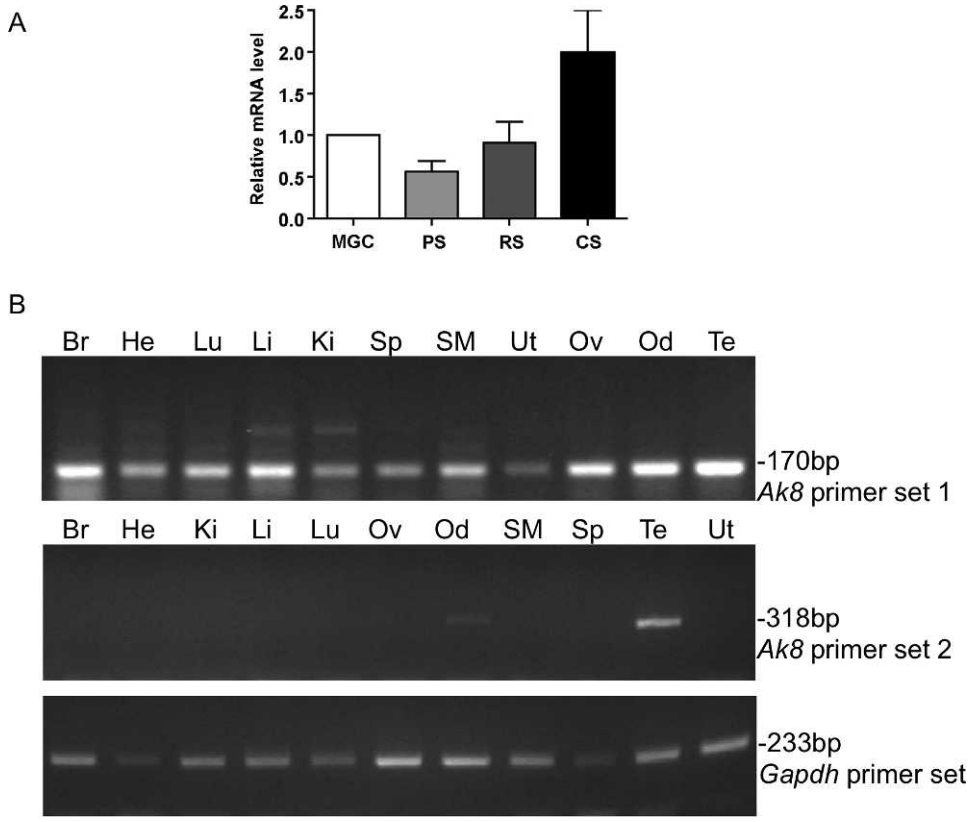

FIG. 6. *Ak8* mRNA expression profile. Quantitative RT-PCR (**A**) and RT-PCR (**B**) were used to determine the *Ak8* expression levels in spermatogenic cells and pattern in various tissues, respectively. *Gapdh* expression was used as a loading control. MGC, mixed germ cells; PS, pachytene spermatocytes; RS, round spermatids; CS, condensing spermatids; Br, brain; He, heart; Ki, kidney; Li, liver; Lu, lung; Ov, ovary; Od, oviduct; SM, skeletal muscle; Sp, spleen; Te, testis; Ut, uterus.

permeabilized bull sperm reactivated with 0.1 mM ATP show a definite reduction in beat frequency and a markedly increased beat amplitude when a 10–40-times excess of ADP (1–4 mM) is added to the reactivation medium. These results are similar to what we have reported here for detergent-modeled mouse sperm in the presence of ADP or ATP plus AMP. However, based on a consideration of the biophysics of the process, Lesich et al. [28] concluded that ADP is directly exerting its effects on the beat by increasing the tenacity of dynein for the B-subtubule of the outer microtubule doublets of the axoneme; they did not consider the possible influence of AMP on the motility patterns, which we have demonstrated in our studies.

In the original article describing the reactivation of detergent-modeled bull sperm motility with ADP, Lindemann and Rikmenspoel [26] noted that bull sperm require low levels of ATP (0.05–1 mM) for mechanical reactivation to be possible and that the ADP-induced motility of bull sperm is blocked by ATP concentrations over 1 mM. Based the theoretical work of Raff and Blum [29], these authors speculated that AK (previously called myokinase) could convert ADP to ATP in their system, but they did not examine this possibility. In 1989, Schoff et al. [27] demonstrated that the transphosphorylation of ADP to ATP occurs in detergent-modeled bull sperm and is blocked by Ap5A. Based on these results, we successfully predicted that either ATP or ADP could drive motility of the detergent-modeled mouse sperm. However, we were surprised to discover that the patterns of motility were different when using either adenine nucleotide: the motility fueled by ADP leads to flagellar beats with greater amplitude and decreased frequency. Moreover, the pattern of movement involves the complete flagellum, not just the distal tip, as seen with ATP alone. On the basis that 1) AK produces one molecule each of ATP and AMP from two molecules of ADP and 2) the ability of ADP to drive the motility of detergent-modeled sperm could be blocked by inhibition of AK by Ap5A, we hypothesized that AMP and not ADP was the true modulator of the waveform, amplitude, and frequency of the flagellar beat observed when detergent-modeled sperm motility is driven by ADP. Our experimental findings when AMP is added with ATP to the reactivation medium strongly support this hypothesis.

At this point, the mechanism whereby AMP modulates the detergent modeled sperm motility is not clear. We initially hypothesized that AMP may be working through AMPK, but our biochemical and pharmacological studies reported here do not support this concept. This is in contrast with the findings in the boar, where AMPK was found to regulate sperm motility and plasma membrane organization [30, 31]. These experiments used ejaculated boar sperm, whereas our experiments employed epididymal mouse sperm, suggesting that there may be species differences and/or distinctions based on the maturation state of the sperm. It is likely that other AMP-regulated processes are involved, including perhaps one or more AMPK-related kinases [32, 33].

Proteins containing AK domains are encoded by many genes in the genome. At least eight different mouse genes encoding AKs have been identified, and all of these transcripts are present in male mouse germ cells [3]. The growing evidence indicates that AKs are positioned in several different locations throughout the sperm. AK1 is associated with the outer microtubular doublets and ODFs of sperm flagella, and AK2 is localized to the mitochondrial sheath in the midpiece [3]. Based on expression patterns in the BioGPS database

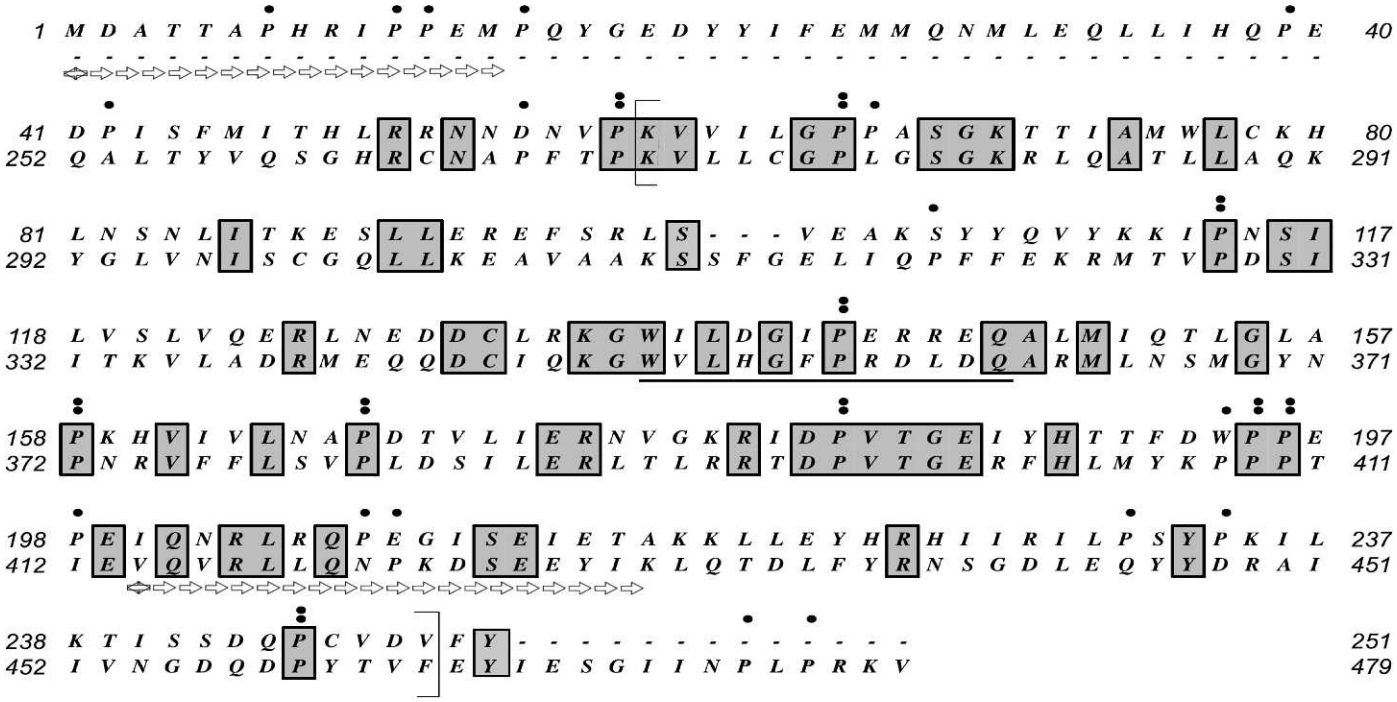

FIG. 7. In silico analysis of the deduced AK8 protein sequence. A protein BLAST analysis as the NCBI server (http://blast.ncbi.nlm.nih.gov/Blast.cgi) identified two AK domains within the AK8 protein sequence [50]. The N-terminal (upper) and C-terminal (lower) portions were aligned to illustrate the two AK regions (brackets corresponding to amino acids 59–249 of the N-terminal portion and 270–463 of the C-terminal domain). The solid line indicates the position of the two regions that align with the canonical signature sequence for AKs. Amino acids conserved between the two AK domains are illustrated with shaded boxes. Prolines are indicated by dots (.) above the sequences; a double dot (:) indicates conserved prolines found in both AK domains. The arrows illustrate the positions of the two peptide sequences (MDATTAPHRIPPEM, amino acids 1–14, and VQVRLLQNPKDSEEYIK, amino acids 414–430) used to generate the AK8 antibody.

(http://biogps.org), three of these genes (*Taf9* [formerly *Ak6*], *Ak7*, and *Ak8*) are preferentially expressed in the testis, raising the possibility that TAF9 and AK7, as we have shown here for AK8, may have very specific functions or localizations in sperm [34]. The known locations of AKs in mouse cauda epididymal sperm and somatic cells are summarized in Table 4.

TABLE 3. Features of adenylate kinase 8 in the mouse.[a]

Amino acid composition	No.	Percentage
Nonpolar		
A	19	3.97
V	29	6.05
L	53	11.06
I	38	7.93
P	37	7.72
M	13	2.71
F	15	3.13
W	4	0.84
Polar		
G	23	4.80
S	25	5.22
T	25	5.22
C	7	1.46
Y	20	4.18
N	20	4.18
Q	26	5.43
Acidic		
D	25	5.22
E	33	6.89
Basic		
K	26	5.43
R	30	6.26
H	11	2.30

[a] Number of amino acids = 479; calculated molecular weight = 55 072.31; estimated pI = 8.34.

Our experiments demonstrate the presence of another compartmentalized AK within sperm. The *Ak8* gene is activated during spermatogenesis, and protein production coincides with flagellar biogenesis. Indirect immunofluorescence localized AK8 to the flagellum and acrosomal region of cauda epididymal sperm (Fig. 9). Triton X-100 treatment extracts membranes and releases soluble cytoplasmic components from cauda epididymal sperm but leaves the flagellar accessory structures and axoneme intact. AK8 was found in the pellet of sperm extracted with 1% Triton X-100 but was released into the supernatant with S-EDTA, which solubilizes additional sperm components, including the axoneme, yet leaves flagellar accessory structures, such as the fibrous sheath, ODFs, and remnants of the mitochondrial sheath, intact. We conclude that AK8 associates with the axoneme and may allow for buffering of ATP among the axoneme and other compartments of the flagellum.

The mechanisms for the association of AK with sperm structures are not known at present. Clearly, there are different processes involved that enable different AK isoforms to be compartmentalized with specific sperm structures (e.g., mitochondria, ODFs, and axonemes). AK8 is rich in prolines that are distributed throughout the primary structure of the protein (Fig. 7). In terms of secondary structure, proline is known as a ''helix breaker'' because the structure of this amino acid causes a rigid kink wherever it resides. In fact, the primary structures of many ligands for protein-protein interactions contain critical prolines [35]. For example, SH3, WW, and several other protein-interaction domains prefer ligand sequences that are proline rich, suggesting that some of the prolines in AK8 may

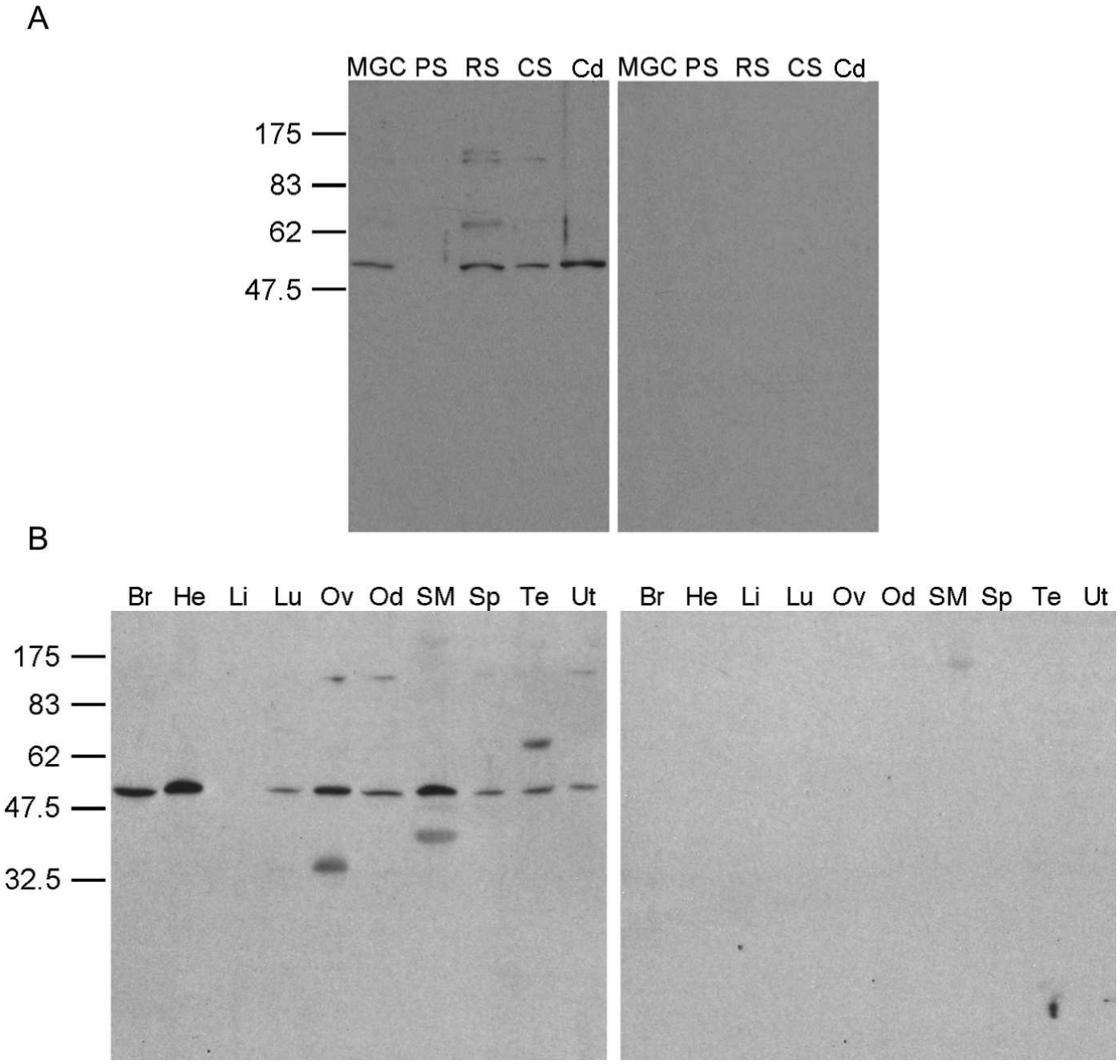

FIG. 8. AK8 protein expression profile. SDS-PAGE and immunoblotting of spermatogenic cells and various tissues was used to determine in which tissues AK8 was present. **A**) AK8 was seen in mixed germ cells, round spermatids, and condensing spermatids. **B**) AK8 was found in all tissues examined except liver. Immunoblots probed with anti-AK8 serum are located on the left. Immunoblots probed with preimmune serum are located on the right. MGC, mixed germ cells; PS, pachytene spermatocytes; RS, round spermatids; CS, condensing spermatids; Cd, cauda epididymal sperm; Br, brain; He, heart; Li, liver; Lu, lung; Ov, ovary; Od, oviduct; SM, skeletal muscle; Sp, spleen; Te, testis; Ut, uterus.

be involved in binding to other proteins of a complex that may buffer energy levels within microdomains of the sperm flagellum.

Flagellar AKs have been well characterized in nonmammalian species. In sperm from the tunicate *Ciona intestinalis*, AK58 possesses two AK domains and is found in the radial spokes of the axoneme [20]. Sea urchin sperm flagella do not possess accessory structures similar to those found in mammalian sperm. However, like AK8 of mouse sperm and AK58 of *Ciona* sperm, Sp-AK has multiple AK domains, is localized along the entire flagellum, and is tightly bound to the axoneme [36]. In trypanosomes, which contain long, complex flagella, seven specific AKs are expressed, and three of these are anchored within two distinct flagellar structures [37]. In *Chlamydomonas reinhardtii*, AK is anchored to the axoneme by a complex that has yet to be fully characterized [38]. In addition, another *Chlamydomonas* protein, Cpc1, is a central pair component and contains an AK domain [39]. Cilia of *Tetrahymena thermophila* possess AK activity, and more than 95% of the total activity was recovered in the axonemal fraction when these cilia were demembranated [40]. These results provide further evidence that members of the AK family are tightly bound to axoneme in the cilia and flagella of many species.

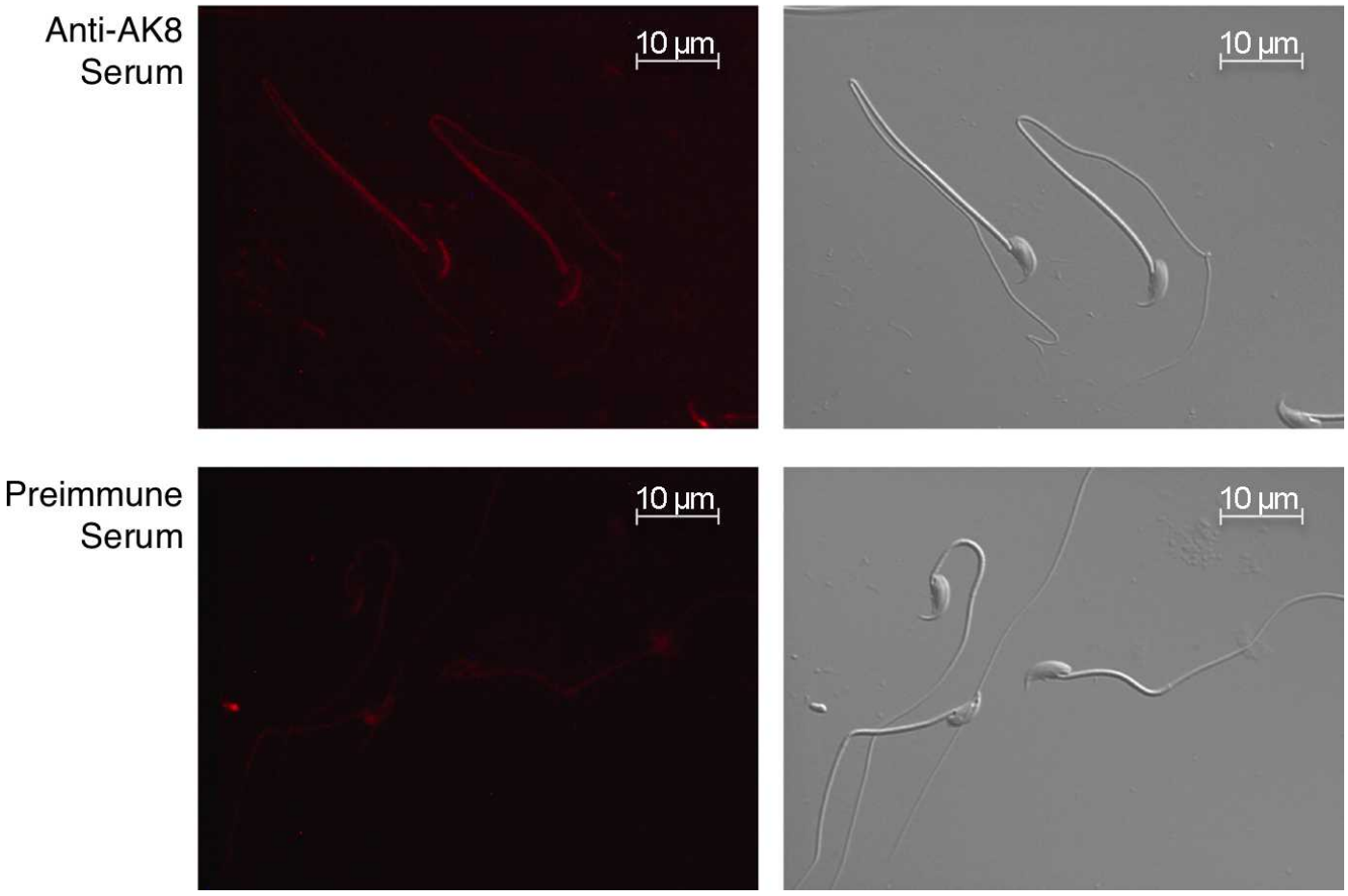

FIG. 9. Localization of AK8 in cauda epididymal sperm. Immunofluorescence of cauda epididymal sperm was performed to determine the localization of AK8 in sperm. AK8 was present along the full length of the sperm tail and the acrosomal region of the sperm head (top). No fluorescence was observed when sperm were probed with preimmune serum (bottom). Nomarski images are located to the right of the fluorescent images. A 10-μm bar is indicated on all images.

Molecular techniques have been used in attempts to interpret the role of the AK enzymes as well as their connections within the flagellum. RNAi has been used to modulate the levels of specific AK forms within trypanosomes. Three of the isoforms were found to be critical for parasite growth; however, there were no reports of the effects of these experiments on flagellar movement [37]. The mouse *Ak1* gene has been deleted by homologous recombination [41]. Although the motility of sperm from these mice has not been examined, the *Ak1*-null mice are still fertile, suggesting that other AK activities may compensate for the lack of AK1. Several other AK enzymes have not been fully characterized in mouse sperm but may also have important functions. For example, AK7 has an essential role and causes primary cilia dyskinesia when mutated [13, 42–44]. In the mouse, the *Ak7* gene was serendipitously mutated by a frame-shift mutation with the result that the male mice are infertile due to the absence of the axonemal central microtubule pair and abnormal spermatogenesis; the few sperm that are recoverable are immotile. It is possible that specific AKs are essential for ciliary and/or flagellar biogenesis; however, the presence of multiple AKs within a fully formed structure may allow for compensation of function in the absence of one of several AK family members.

Revisiting Atkinson's [8] model of adenylate energy charge provides a framework for addressing these issues. As ATP is consumed for energy-requiring processes or for signaling

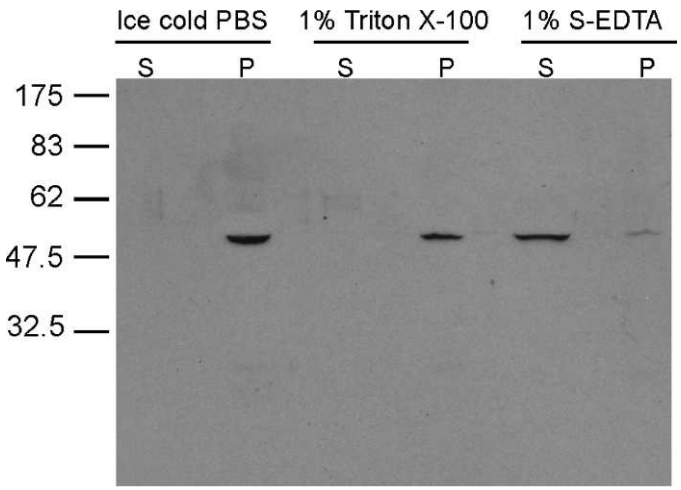

FIG. 10. Detergent fractionation of cauda epididymal sperm. A series of detergent extractions was performed on cauda epididymal sperm to determine if AK8 was associated with the sperm axoneme. Sperm were extracted in ice-cold PBS, 1% Triton X-100, and 1% S-EDTA. Supernatants (S) were separated from pellets (P). Samples were further processed for SDS-PAGE and immunoblotting.

TABLE 4. Known locations for adenylate kinases in mouse sperm.

Protein	Location in somatic cells	Expression in MGCs*	Location in sperm [reference]†
AK1	Cytoplasm	Yes	Flagellum: ODF [8]
AK2	Mitochondrial compartments	Yes	Flagellum: mitochondrial sheath [8]
AK3	Mitochondrial compartments	Yes	?
AK4	Mitochondrial compartments	Yes	?
AK5	Cytoplasm	Yes	?
TAF9 (AK6)	Nucleus	Yes	?
AK7	Cytoplasm	Yes	Flagellum: axoneme [9]
AK8	Cytoplasm	Yes	Flagellum: acrosome [present study]

* Messenger RNAs for all eight AKs are present in male mouse mixed germ cells (MGCs) [3].
† AK1, AK2, and AK8 have been characterized in cauda epididymal mouse sperm.

through phosphorylation, ADP will be generated. When the consumption of ATP exceeds its generation, the cell still has the capacity to produce one molecule of ATP from two molecules of ADP, consequentially producing a molecule of AMP. At the same time, adenylyl cyclases use ATP production of cAMP, which serves in its own signaling capacity [45, 46]. Cyclic AMP, in turn, is degraded to AMP by phosphodiesterase activity [47]. This raises the possibility that phosphodiesterase serves as a switch from cAMP-based to AMP-dependent signaling. Curiously, the major adenylyl cyclase of mouse sperm, the so-called soluble adenylyl cyclase (ADCY10), is compartmentalized in the midpiece of the sperm flagellum [46].

The fact that the inclusion of AMP with ATP recapitulated the pattern seen with ADP alone in detergent-permeabilized sperm is significant and raises important, new issues concerning the compartmentalization of metabolic processes and the regulation of motility in intact sperm. Several studies have demonstrated that many enzymes of the glycolytic pathway are localized in the principal piece of the sperm flagellum, while oxidative phosphorylation occurs within the mitochondria-rich midpiece [1, 18, 48]. Furthermore, enzymes such as adenylyl cyclase (ADCY10) and phosphodiesterases (PDEs) are compartmentalized in different regions of the intact sperm cell [12, 46, 49]. Buffering of ATP levels throughout the tail or shuttling of ADP and ATP equivalents up and down the flagellum of intact sperm could be mediated, in part, by compartmentalized AK activity [3]. As a consequence, the respective levels of ATP, ADP, and AMP with a given region of the flagellum of intact sperm could result in dynamic regulation of energy-requiring processes and signaling events. We propose that the relative ratios of adenine nucleotides (ATP, ADP, AMP, and cAMP) and the compartmentalized locations of enzymes (AK, ADCY10, PDEs, and so on) in intact sperm are key to understanding the processes fueling and regulating sperm flagellar motion.

ACKNOWLEDGMENT

We would like to thank the members of the Gerton laboratory for their encouragement and support of this project. We also appreciate the assistance of Roger Ladewig with the analysis of flagellar angularity.

REFERENCES

1. Krisfalusi M, Miki K, Magyar PL, O'Brien DA. Multiple glycolytic enzymes are tightly bound to the fibrous sheath of mouse spermatozoa. Biol Reprod 2006; 75(2):270–278.
2. Nakamura N, Dai Q, Williams J, Goulding EH, Willis WD, Brown PR, Eddy EM. Disruption of a spermatogenic cell-specific mouse Enolase 4 (Eno4) gene causes sperm structural defects and male infertility. Biol Reprod 2013; 88(4):90.
3. Cao W, Haig-Ladewig L, Gerton GL, Moss SB. Adenylate kinases 1 and 2 are part of the accessory structures in the mouse sperm flagellum. Biol Reprod 2006; 75(4):492–500.
4. Visconti PE, Krapf D, de la Vega-Beltran JL, Acevedo JJ, Darszon A. Ion channels, phosphorylation and mammalian sperm capacitation. Asian J Androl 2011; 13(3):395–405.
5. Vadnais ML, Aghajanian HK, Lin A, Gerton GL. Signaling in sperm: toward a molecular understanding of the acquisition of sperm motility in the mouse epididymis. Biol Reprod 2013; 89(5):127, 1–10.
6. Navarro B, Miki K, Clapham DE. ATP-activated P2X2 current in mouse spermatozoa. PNAS 2011; 108(34):14342–14347.
7. Burton KA, McKnight GS. PKA, germ cells, and fertility. Physiology (Bethesda) 2007; 22:40–46.
8. Atkinson DE. Energy charge of the adenylate pool as a regulatory parameter. Interaction with feedback modifiers. Biochemistry 1968; 7(11): 4030–4034.
9. Kamp G, Schmidt H, Stypa H, Feiden S, Mahling C, Wegener G. Regulatory properties of 6-phosphofructokinase and control of glycolysis in boar spermatozoa. Reproduction 2007; 133(1):29–40.
10. Fogarty S, Hardie DG. Development of protein kinase activators: AMPK as a target in metabolic disorders and cancer. Biochim Biophys Acta Proteins Proteomics 2010; 1804(3):581–591.
11. McGee SL, Hargreaves M. AMPK-mediated regulation of transcription in skeletal muscle. Clin Sci 2010; 118(8):507–518.
12. Bajpai M, Fiedler SE, Huang Z, Vijayaraghavan S, Olson GE, Livera G, Conti M, Carr DW. AKAP3 selectively binds PDE4A isoforms in bovine spermatozoa. Biol Reprod 2006; 74(1):109–18.
13. Fernandez-Gonzalez A, Kourembanas S, Wyatt TA, Mitsialis SA. Mutation of murine adenylate kinase 7 underlies a primary ciliary dyskinesia phenotype. Am J Respir Cell Mol Biol 2009; 40(3):305–313.
14. Randak CO, Welsh MJ. Role of CFTR's intrinsic adenylate kinase activity in gating of the Cl– channel. J Bioenerg Biomembr 2007; 39(5–6): 473–479.
15. Bellvé AR, Millette CF, Bhatnagar YM, O'Brien DA. Dissociation of the mouse testis and characterization of isolated spermatogenic cells. J Histol Cytochem 1977; 25(7):480–494.
16. Gerton GL, Millette CF. Generation of flagella by cultured mouse spermatids. J Cell Biol 1984; 98(2):619–628.
17. Romrell LJ, Bellvé AR, Fawcett DW. Separation of mouse spermatogenic cells by sedimentation velocity. A morphological characterization. Dev Biol 1976; 49(1):119–131.
18. Travis AJ, Jorgez CJ, Merdiushev T, Jones BH, Dess DM, Diaz-Cueto L, Storey BT, Kopf GS, Moss SB. Functional relationships between capacitation-dependent cell signaling and compartmentalized metabolic pathways in murine spermatozoa. J Biol Chem 2001; 276(10):7630–7636.
19. Livak KJ, Schmittgen TD. Analysis of relative gene expression data using real-time quantitative PCR and the 2(-delta delta C(T)) method. Methods 2001; 25(4):402–408.
20. Jeong Y-J, Choi H-W, Shin H-S, Cui X-S, Kim N-H, Gerton GL, Jun JH. Optimization of real time RT-PCR methods for the analysis of gene expression in mouse eggs and preimplantation embryos. Mol Reprod Dev 2005; 71(3):284–289.
21. Laemmli UK. Cleavage of structural proteins during the assembly of the head of bacteriophage T4. Nature 1970; 227(5259):680–685.
22. Towbin H, Staehelin T, Gordon J. Electrophoretic transfer of proteins from polyacrylamide gels to nitrocellulose sheets: procedure and some applications. Proc Natl Acad Sci U S A 1979; 76(9):4350–4354.
23. ExPASy Bioinformatics Resource Portal [Internet]. Lausanne, Switzerland: Swiss Institute of Bioinformatics. http://prosite.expasy.org/PDOC00104. Accessed 27 July 2013.
24. Cao W, Gerton GL, Moss SB. Proteomic profiling of accessory structures

from the mouse sperm flagellum. Mol Cell Proteomics 2006; 5(5): 801–810.
25. Carrera A, Gerton GL, Moss SB. The major fibrous sheath polypeptide of mouse sperm: structural and functional similarities to the A-kinase anchoring proteins. Dev Biol 1994; 165(1):272–284.
26. Lindemann CB, Rikmenspoel R. Sperm flagellar motion maintained by ADP. Exp Cell Res 1972; 73(1):255–259.
27. Schoff PK, Cheetham J, Lardy HA. Adenylate kinase activity in ejaculated bovine sperm flagella. J Biol Chem 1989; 264:6086–6091.
28. Lesich KA, Pelle DW, Lindemann CB. Insights into the mechanism of ADP action on flagellar motility derived from studies on bull sperm. Biophys J 2008; 95(1):472–482.
29. Raff EC, Blums JJ. A possible role for adenylate kinase in cilia: concentration profiles in a geometrically constrained dual enzyme system. J Theor Biol 1968; 18(1):53–71.
30. Hurtado de Llera A, Martin-Hidalgo D, Gil MC, Garcia-Marin LJ, Bragado MJ. AMP-activated kinase AMPK is expressed in boar spermatozoa and regulates motility. PLoS ONE 2012; 7(6):e38840.
31. Hurtado de Llera A, Martin-Hidalgo D, Rodriguez-Gil JE, Gil MC, Garcia-Marin LJ, Bragado MJ. AMP-activated kinase, AMPK, is involved in the maintenance of plasma membrane organization in boar spermatozoa. Biochim Biophys Acta Biomembr 2013; 1828(9):2143–2151.
32. Bright NJ, Thornton C, Carling D. The regulation and function of mammalian AMPK-related kinases. Acta Physiol 2009; 196(1):15–26.
33. Xu B, Hao Z, Jha KN, Digilio L, Urekar C, Kim YH, Pulido S, Flickinger CJ, Herr JC. Validation of a testis specific serine/threonine kinase [TSSK] family and the substrate of TSSK1 & 2, TSKS, as contraceptive targets. Soc Reprod Fertil Suppl 2007; 63:87–101.
34. BioGPS [Internet]. LaJolla, CA: The Scripps Research Institute. http://biogps.org/BioGPS. Accessed 04 June 2013.
35. Kay BK, Williamson MP, Sudol M. The importance of being proline: the interaction of proline-rich motifs in signaling proteins with their cognate domains. FASEB J 2000; 14(2):231–241.
36. Kinukawa M, Nomura M, Vacquier VD. A sea urchin sperm flagellar adenylate kinase with triplicated catalytic domains. J Biol Chem 2007; 282(5):2947–2955.
37. Ginger ML, Ngazoa ES, Pereira CA, Pullen TJ, Kabiri M, Becker K, Gull K, Steverding D. Intracellular positioning of isoforms explains an unusually large adenylate kinase gene family in the parasite *Trypanosoma brucei*. J Biol Chem 2005; 280(12):11781–11789.
38. Wirschell M, Pazour G, Yoda A, Hirono M, Kamiya R, Witman GB. Oda5p, a novel axonemal protein required for assembly of the outer dynein arm and an associated adenylate kinase. Mol Biol Cell 2004; 15(6): 2729–2741.
39. Zhang H, Mitchell DR. Cpc1, a Chlamydomonas central pair protein with an adenylate kinase domain. J Cell Sci 2004; 117(pt 18):4179–4188.
40. Nakamura K, Iitsuka K, Fujii T. Adenylate kinase is tightly bound to axonemes of Tetrahymena cilia. Comp Biochem Physiol B Biochem Mol Biol 1999; 124(2):195–199.
41. Janssen E, Dzeja PP, Oerlemans F, Simonetti AW, Heerschap A, de Haan A, Rush PS, Terjung RR, Wieringa B, Terzic A. Adenylate kinase 1 gene deletion disrupts muscle energetic economy despite metabolic rearrangement. EMBO J 2000; 19(23):6371–6381.
42. Mata M, Lluch-Estellés J, Armengot M, Sarrión I, Carda C, Cortijo J. New adenylate kinase 7 (AK7) mutation in primary ciliary dyskinesia. Am J Rhinol Allergy 2012; 26(4):260–264.
43. Milara J, Armengot M, Mata M, Morcillo EJ, Cortijo J. Role of adenylate kinase type 7 expression on cilia motility: possible link in primary ciliary dyskinesia. Am J Rhinol Allergy 2010; 24(3):181–185.
44. Vogel P, Read RW, Hansen GM, Payne BJ, Small D, Sands AT, Zambrowicz BP. Congenital hydrocephalus in genetically engineered mice. Vet Pathol 2012; 49(1):166–181.
45. Esposito G, Jaiswal BS, Xie F, Krajnc-Franken MAM, Robben TJAA, Strik AM, Kuil C, Philipsen RLA, van Duin M, Conti M, Gossen JA. Mice deficient for soluble adenylyl cyclase are infertile because of a severe sperm-motility defect. Proc Natl Acad Sci U S A 2004; 101(9):2993–2998.
46. Hess KC, Jones BH, Marquez B, Chen Y, Ord TS, Kamenetsky M, Miyamoto C, Zippin JH, Kopf GS, Suarez SS, Levin LR, Williams CJ, et al. The ''soluble'' adenylyl cyclase in sperm mediates multiple signaling events required for fertilization. Dev Cell 2005; 9(2):249–259.
47. Fisch JD, Behr B, Conti M. Enhancement of motility and acrosome reaction in human spermatozoa: differential activation by type-specific phosphodiesterase inhibitors. Hum Reprod 1998; 13(5):1248–1254.
48. Mukai C, Okuno M. Glycolysis plays a major role for adenosine triphosphate supplementation in mouse sperm flagellar movement. Biol Reprod 2004; 71(2):540–547.
49. Baxendale RW, Fraser LR. Mammalian sperm phosphodiesterases and their involvement in receptor-mediated cell signaling important for capacitation. Mol Reprod Dev 2005; 71(4):495–508.
50. Basic Local Alignment Search Tool [Internet]. Bethesda, MD: National Library of Medicine. http://blast.ncbi.nlm.nih.gov/Blast.cgi. Accessed 06 August 2013.